Trimetallic Nitride Template Endohedral Metallofullerenes: Discovery, Structural Characterization, Reactivity, and Applications

JIANYUAN ZHANG,[†] STEVEN STEVENSON,[*,‡] AND
HARRY C. DORN[*, †, §]

[†]Department of Chemistry, Virginia Polytechnic Institute and State University, Blacksburg, Virginia 24061, United States, [‡]Depart of Chemistry, Indiana University−Purdue University Fort Wayne, 2101 E Coliseum Boulevard, Fort Wayne, Indiana 46805, United States, and [§]Virginia Tech Carilion Research Institute, Roanoke, Virginia 24016, United States

CONSPECTUS

Shortly after the discovery of the carbon fullerene allotrope, C_{60}, researchers recognized that the hollow spheroidal shape could accommodate metal atoms, or clusters, which quickly led to the discovery of endohedral metallofullerenes (EMFs). In the past 2 decades, the unique features of EMFs have attracted broad interest in many fields, including inorganic chemistry, organic chemistry, materials chemistry, and biomedical chemistry. Some EMFs produce new metallic clusters that do not exist outside of a fullerene cage, and some other EMFs can boost the efficiency of magnetic resonance (MR) imaging 10−50-fold, in comparison with commercial contrast agents. In 1999, the Dorn laboratory discovered the trimetallic nitride template (TNT) EMFs, which consist of a trimetallic nitride cluster and a host fullerene cage. The TNT-EMFs ($A_3N@C_{2n}$, $n = 34−55$, A = Sc, Y, or lanthanides) are typically formed in relatively high yields (sometimes only exceeded by empty-cage C_{60} and C_{70}, but yields may decrease with increasing TNT cluster size), and exhibit high chemical and thermal stability.

In this Account, we give an overview of TNT-EMF research, starting with the discovery of these structures and then describing their synthesis and applications. First, we describe our serendipitous discovery of the first member of this class, $Sc_3N@I_h$-C_{80}. Second, we discuss the methodology for the synthesis of several TNT-EMFs. These results emphasize the importance of chemically adjusting plasma temperature, energy, and reactivity (CAPTEAR) to optimize the type and yield of TNT-EMFs produced. Third, we review the approaches that are used to separate and purify pristine TNT-EMF molecules from their corresponding product mixtures. Although we used high-performance liquid chromatography (HPLC) to separate TNT-EMFs in early studies, we have more recently achieved facile separation based on the reduced chemical reactivity of the TNT-EMFs. These improved production yields and separation protocols have allowed industrial researchers to scale up the production of TNT-EMFs for commercial use. Fourth, we summarize the structural features of individual members of the TNT-EMF class, including cage structures, cluster arrangement, and dynamics. Fifth, we illustrate typical functionalization reactions of the TNT-EMFs, particularly cycloadditions and radical reactions, and describe the characterization of their derivatives. Finally, we illustrate the unique magnetic and electronic properties of specific TNT-EMFs for biomedicine and molecular device applications.
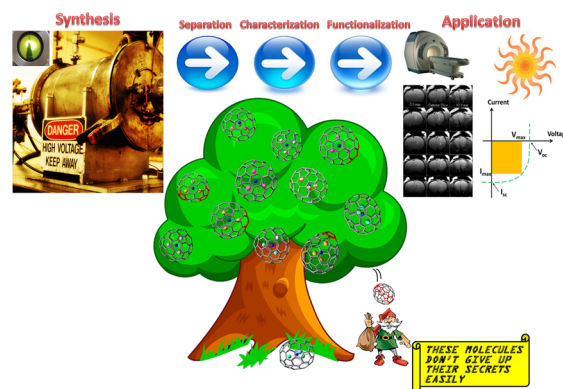
1. Discovery of Trimetallic Nitride Templated Endohedral Metallofullerenes (TNT-EMFS)

Shortly after the discovery of the C_{60} molecule,[1] it was recognized that encapsulation of atoms, ions, and clusters inside fullerene cages was feasible. Since the 1990s, a number of mono- and dimetallic metallofullerenes were reported, as described in a recent Account by Akasaka and co-workers.[2] During the 1990s, the Dorn Virginia Tech laboratory engaged in studies of these endohedral fullerenes. For the case of scandium metallofullerenes, our

laboratory consistently observed a mass spectral peak at $m/e = 1109$ (with variable intensity) for the toluene-soluble soot product, prepared utilizing a Krätschmer—Huffman (K—H) reactor electric-arc reactor (*vide infra*).[3] Although the mass spectral 1109 peak appeared in early reports, it remained unidentified.[4] During this time period, Whetten and co-workers[5] proposed the possibility of I_h-C_{80} or D_{5h}-C_{80} fullerene structures for the dimetallic endohedral metallofullerene $La_2@C_{80}$. Akasaka and co-workers had reported the ^{13}C and ^{139}La NMR spectra for $La_2@C_{80}$, which was also consistent with an I_h-C_{80} cage.[6] In the fall of 1998, Stevenson and Dorn, armed with reams of data files (i.e., mass spectral data, isotope distribution tables, ^{45}Sc NMR spectrum, and chromatographic traces), spent several hours at a local coffee shop and concluded that, based on the mass spectral isotopic distribution for the ^{13}C enriched sample, the mysterious molecular formula for the 1109 peak was $Sc_3C_{80}N_1$, representing a four-atom endohedral cluster inside an I_h-C_{80} cage, namely, $Sc_3N@I_h$-C_{80} (Figure 1). This structure assumed that three Sc^{3+} ions and an N^{3-} ion contribute a total of six electrons to stabilize the I_h-C_{80} fullerene cage, I_h-C_{80}^{6-}, as predicted by Whetten and Akasaka.[5,6] The occurrence of a nitrogen atom in the formula was completely unexpected since no nitrogen-containing precursor was used as a starting material (helium gas, graphite, and scandium oxide). This epiphany was subsequently confirmed by a two-line pattern obtained for the 150 MHz ^{13}C NMR spectrum (Figure 1), which required nearly 1 week of scan time utilizing a 600 MHz (14.1 T) NMR instrument (Roy Bible, G. D. Searle). The simple two-line pattern reflects the two types of carbon atoms in a characteristic 3:1 ratio (60×1, 20×1) for I_h-C_{80} symmetry. Moreover, the ^{13}C NMR spectrum for the ^{13}C-enriched sample exhibited a significantly enhanced doublet $^1J_{C-C}$ coupling pattern for the smaller peak, consistent with an sp^2 carbon signal coupled to three equivalent adjacent carbons. With this new data, our suspicion was that the nitrogen source was from an air leak into the K—H chamber. This was confirmed in new experiments by intentionally introducing nitrogen gas into the chamber, which led to a significant increase in the level of the TNT-EMF $Sc_3N@I_h$-C_{80}.[7] With larger sample quantities, we were able to isolate a sufficient sample (still less than 1 mg) for an elegant single-crystal X-ray study by Alan Balch's laboratory, unambiguously confirming the structure. This serendipitous discovery was seemingly more predetermined when we realized that the Dorn Virginia Tech office number was the same as the formula mass of $Sc_3N@I_h$-C_{80} (Hahn 1109).
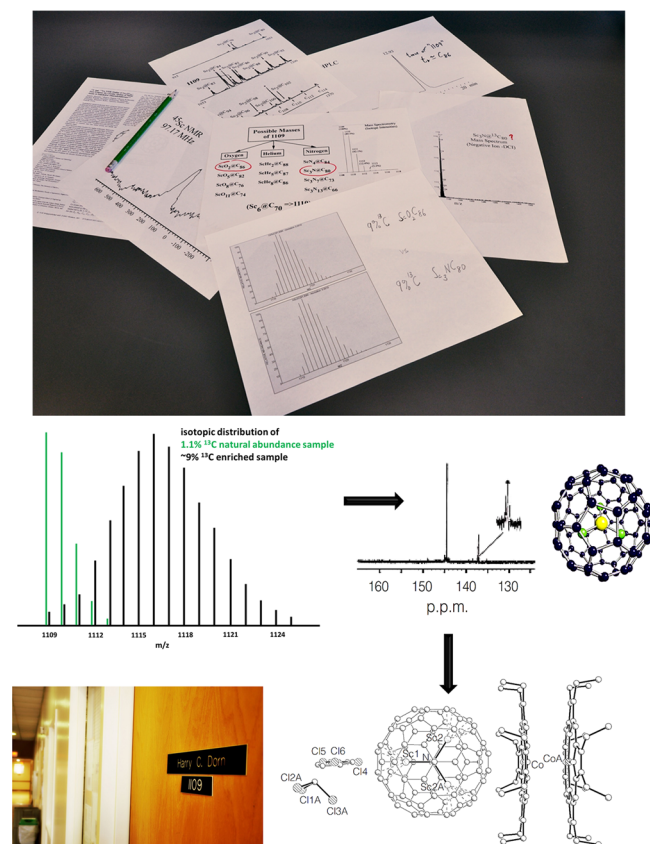

FIGURE 1. Discovery of TNT-EMFs: (top) spectral data and reference papers leading to the discovery of "1109", $Sc_3N@C_{80}$; (bottom) mass spectral isotopic distribution of natural abundance and ^{13}C-enriched $Sc_3N@C_{80}$; the ^{13}C NMR and single X-ray crystallographic structural data for $Sc_3N@C_{80}$; H.C.D.'s Virginia Tech office number, Hahn Hall 1109.

It was later found that the protypical scandium member, $Sc_3N@I_h$-C_{80}, was significantly stabilized by formal transfer of six electrons to the icosahedral I_h cage, C_{80}^{6-}.[8,9] It was also quickly recognized that other fullerene cages would accommodate the Sc_3N cluster, including a second isomer for the C_{80} cage, $Sc_3N@D_{5h}$-C_{80}, a slightly smaller cage, $Sc_3N@D_{3h}$-C_{78}, and a non-isolated pentagon rule (non-IPR) structure, $Sc_3N@D_3$-C_{68}. These new TNT-EMFs have also been characterized by both ^{13}C NMR and single-crystal studies. With yttrium and lanthanide metal ions, a whole family of TNT-EMFs, $A_3N@C_{2n}$ (A = Sc, Y, Gd, Tb, Dy, Ho, Er, Tm, Lu, Pr, Ce, and La, $n = 34$, 35, and 39−55), have been produced and characterized in the laboratories of Dorn, Echegoyen, Balch, Dunsch, Stevenson, Yang, and others. The TNT-EMF family also allows "mixed" metal formation, $A_xB_{3-x}N@C_{2y}$ ($x = 0-3$, A, B = metal).[7] In early studies, a series of mixed-metal syntheses were performed, and the yield of $Sc_xA_{3-s}@C_{80}$ was shown relative to Sc_2C_{84} based on mass-spectrometry peak intensity (Figure 2b). As a general
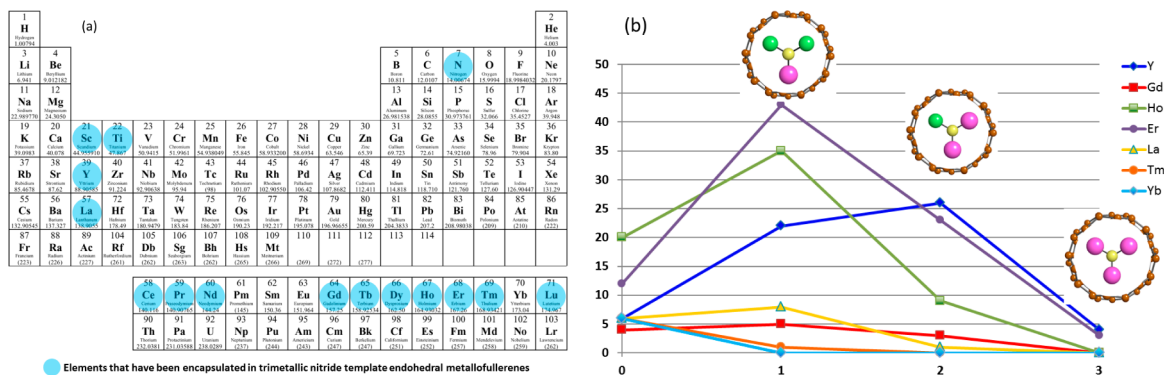
FIGURE 2. (a) Elements that have been encapsulated in TNT-EMFs. (b) Relative mass-spectrometry peak intensity of mixed-metal TNT-EMFs $Sc_xA_{3-x}N@C_{80}$ to Sc_2C_{84}.
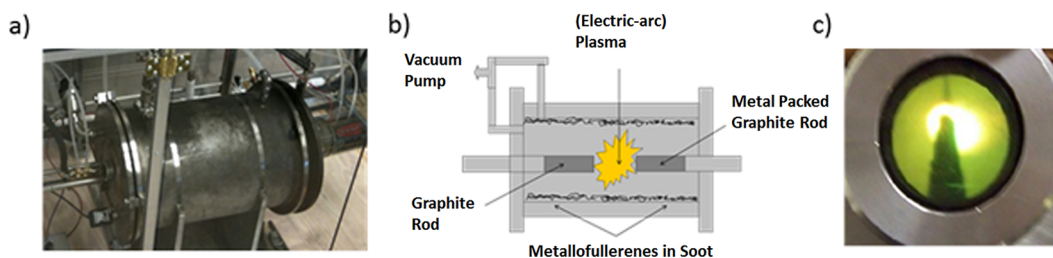

FIGURE 3. (a) An electric-arc reactor (chamber size about 30 cm in diameter and 60 cm in length) and (b) drawing. (c) The plasma.

trend, for both homogeneous and mixed-metal TNT-EMFs, the yield of a certain species decreases as cluster size increases.[10] An earlier review of TNT-EMFs have been published by Dunsch,[9] and recent development of TNT-EMFs are also described in other EMF reviews by Echegoyen,[11] Balch,[12] and Akasaka[10,13] with their collaborators.

2. Preparation of TNT-EMFs

In most preparations to date, TNT-EMFs are produced in a K−H electric-arc reactor.[3] Although the geometrical dimensions of the K−H reactor vary, a typical apparatus is shown in Figure 3a,b. The soot containing the TNT-EMFs is produced from the electric-arc vaporization of a core-drilled graphite rod packed with the desired metal to be encapsulated. The resulting arc plasma in operation is shown in Figure 3c.

In the K−H production method, the TNT-EMFs are prepared by vaporizing graphite rods packed with the metal oxide (e.g., Sc_2O_3) in ~100−300 Torr atmosphere of N_2 and He.[7] The soot obtained from the K−H reactor contains predominantly empty-cage fullerenes (e.g., C_{60}, C_{70}), which need to be removed during the purification process *vide infra*. Subsequently, a more reactive gas atmosphere was reported by Dunsch,[14] who introduced NH_3 into the K−H reactor. The Dunsch method, and its reducing atmosphere, provided

samples depleted in C_{60} and C_{70} and enriched in TNT-EMFs. In later studies, an oxidizing atmosphere was reported by Stevenson,[15] who introduced O_2 and NO_x vapor via the decomposition of $Cu(NO_3)_2$, which was added to metal-packed rods prior to vaporization. The Stevenson laboratory has shown that the yield can be increased by 3−5 times in the presence of Cu.[16] As an example of the types of EMFs that can be made by the CAPTEAR method,[15] Figure 4a shows laser desorption/ionization time-of-flight (LDI-TOF) mass spectral results from soot extracts, which emphasize the production of larger lanthanum−scandium mixed-metal clusters. The mixed-metal $LaSc_2N@C_{80}$ TNT-EMF and corresponding $LaSc_2N@C_{79}N$ are the dominant species under these conditions. Although the dilanthanum species of $La_2ScN@C_{80}$ and $La_2ScN@C_{79}N$ are synthesized in much lower yields, the large cluster, $La_3N@C_{80}$, is below mass spectral limits of detection. Surprisingly, the TNT heterofullerene $La_3N@C_{79}N$ is also formed.[17]

3. Purification of TNT-EMFs

The first TNT-EMFs were isolated and purified by high-performance liquid chromatography (HPLC), but these efforts are time-consuming and limit the quantities of TNT-EMFs that can be isolated in pure form. It was, however, found that TNT-EMFs have significantly different chemical
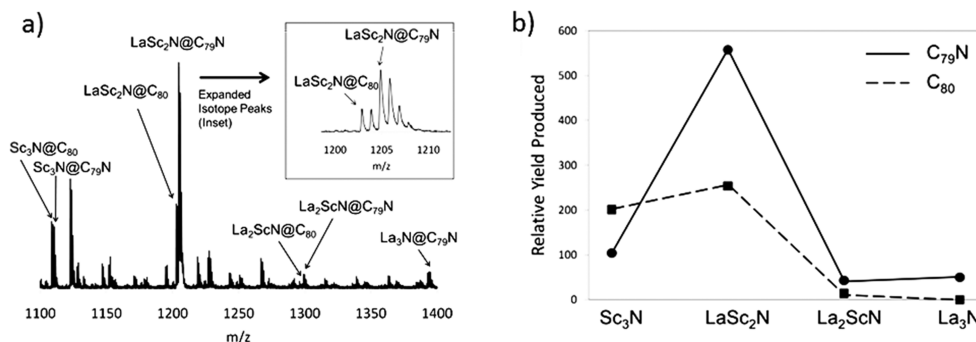
FIGURE 4. (a) LDI-TOF of CAPTEAR produced fullerene extract and (b) plot showing the relative yields of TNT-EMFs versus TNT-MNAFs.
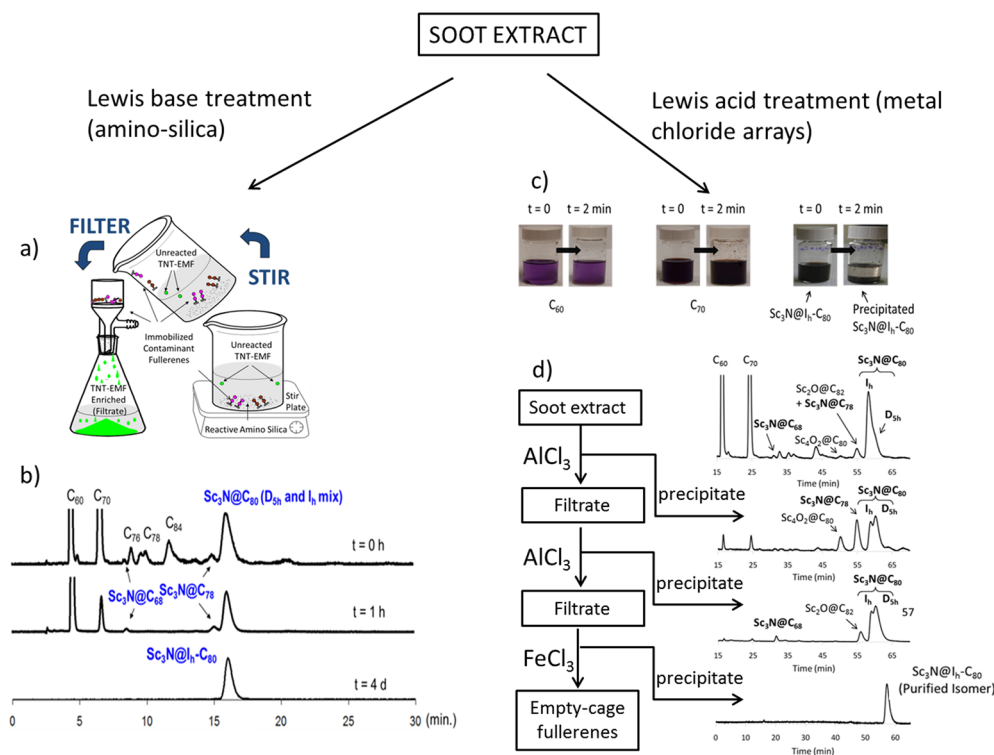

FIGURE 5. Lewis acid and base reactivity separations of TNT-EMFs.

reactivities than empty-cage fullerenes.[18−22] For example, a facile separation of TNT-EMFs was reported based on lower Diels−Alder chemical reactivity of TNT-EMFs between a cyclopentadiene moiety immobilized on silica gel in comparison with empty-cage fullerenes.[18] One of the more facile separations reported to date is the treatment with either Lewis bases or Lewis acids to selectively bind the more reactive species (Figure 5). As a typical example, via the "stir and filter approach" (SAFA, Figure 5a) developed by Stevenson et al,[19,20] empty-cage fullerenes bind readily to amino-derivitized silica (Lewis base) with the more chemically inert TNT-EMFs remaining in solution. However, the most unreactive component, $Sc_3N@I_h$-C_{80}, is readily isolated in isomeric

purity simply by filtration (figure 5b).[19] In contrast, when Lewis acid metal chlorides dissolved in CS_2 are employed (and after stirring), the EMFs were selectively isolated as insoluble complexes (Figure 5c), which can be recovered after decomposing the complexes (in ice water) as pure TNT-EMFs, $Sc_3N@I_h$-C_{80} (Figure 5d).[20]

4. Structural and Computational Studies of TNT-EMFs

As previously described, the first definitive structural confirmation of the TNT-EMF, $Sc_3N@I_h$-C_{80}, was obtained by both single-crystal analysis and ^{13}C NMR spectroscopy.[7] For the I_h-C_{80} cage, although it commonly encapsulates planar

Sc₃N@I_h-C₈₀   Sc₃N@D_{3h}-C₇₈

Sc₃N@D_3-C₆₈   Gd₃N@C_2-C₇₈

Gd₃N@C_s-C₈₂   Gd₃N@C_s-C₈₄

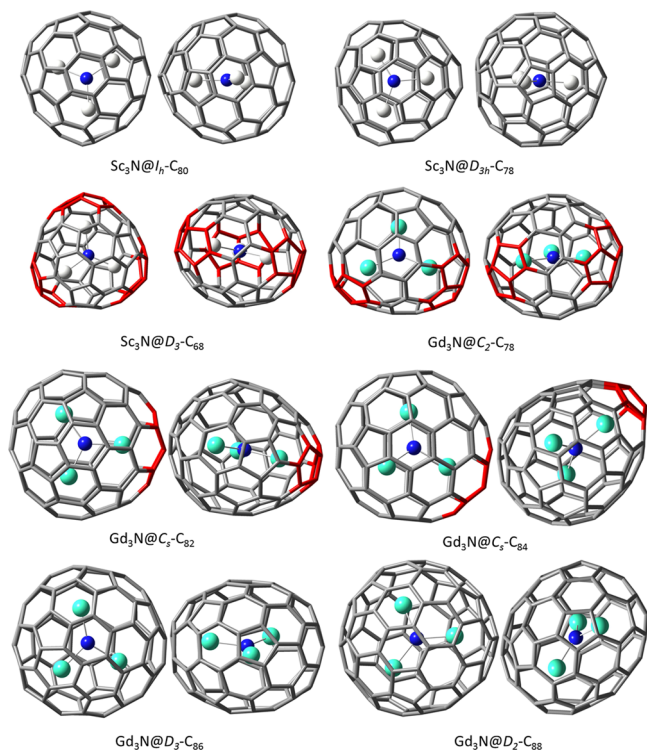Gd₃N@D_3-C₈₆   Gd₃N@D_2-C₈₈

FIGURE 6. Structures of TNT-EMFs based on single-crystal analysis. The red portion of the molecules denotes pentalene site.

A_3N^{6+} clusters, deviations from triangular planarity are observed for larger lanthanide atoms. For example, a cluster that deviates strongly from planarity was found for Gd₃N@I_h-C₈₀, in which the N atom deviates from the trigadolinium plane by a distance of ∼0.5 Å, forming an ammonia-like pyramid.[23] Several other different cage members of the TNT-EMF class have characteristic structural features that are rarely seen in other fullerenes and metallofullerenes (Figure 6). For the C₇₈ cage, two isomeric fullerene cages are found for the trimetallic nitride $(A_3N)^{6+}$ cluster. One is the D_{3h}-C₇₈ cage, represented by Sc₃N@D_{3h}-C₇₈,[24] which is unique for the smaller $(Sc_3N)^{6+}$ cluster and different from any other reported empty-cage C₇₈ fullerene. Larger lanthanide metals including Gd, Tm, Dy, and Y prefer the non-IPR A₃N@C_2(22010)-C₇₈ cage,[25−27] which has a "flatter flying saucer" shape to host larger planar clusters.[26] These larger clusters conserve planarity in place of pyramidalization and thereby stabilize these molecules by 140−160 kJ/mol.[25] The A₃N cluster also adopts a non-IPR C₈₂ cage, namely, the C_s(39663)-C₈₂ cage, as found in the single-crystal structure of Gd₃N@C₈₂, where one of the Gd^{3+} ions was close to the site of the fused pentagons.[28] The non-IPR A₃N@C₈₂ system was confirmed by the ¹³C NMR study of Y₃N@C₈₂, in which a highly deshielded ¹³C signal was observed at 165.7 ppm,

corresponding to the two carbon atoms fusing the pentalene unit.[29] Also noteworthy is that major isomers of all A₃N@C₈₄ (A = Tb, Tm, Gd, or Y) EMFs adopt an egg-shaped non-IPR C_s cage, the C_s(51365)-C₈₄.[29−31] The special elliptical shape of the cage is capable of hosting the planar $(A_3N)^{6+}$ cluster, and the only pentalene group is located on the "tip" of this "buckyegg". The ¹³C NMR results of Y₃N@C₈₄ also confirm the cage symmetry and the existence of the fused pentagons.[29] The reported A₃N@C₈₆ species, where A includes Tb, Gd, and Y, share the same fullerene cage, namely, the D_3(19)-C₈₆, as found by single-crystal X-ray crystallography[32,33] and ¹³C NMR analysis.[29] The A₃N@C₈₈ EMFs are the largest TNT-EMFs with crystal structures reported to date where the D_2(35)-C₈₈ cage is the common host for Tb₃N, Gd₃N, and Y₃N clusters.[32,34]

The smallest and largest isolated TNT-EMFs are Sc₃N@C₆₈[35] and A₃N@C₉₆ (A = Pr, Ce, and La),[36] respectively. The 12 peaks in the ¹³C NMR spectrum of Sc₃N@C₆₈ and symmetric single ⁴⁵Sc signal suggested a D_3-C₆₈ cage, which was confirmed by single-crystal study.[37] Regarding the larger TNT-EMFs in the soot extract for a lanthanum-based TNT-EMF synthesis, a mass-spectral peak corresponding to La₃N@C₁₁₀ was observed, which represents the largest TNT-EMF reported to date.[36]

NMR investigations of the nuclei of the $(A_3N)^{6+}$ cluster provide additional information regarding cluster dynamics. The ⁸⁹Y NMR of Y₃N@C_{2n} (*n* = 40, 42, and 43) series reveals that, in the non-IPR Y₃N@C_s(51365)-C₈₄, the pentalene group strongly binds to one yttrium atom and prevents the cluster rotation, whereas in IPR-obeying Y₃N@C₈₀ and Y₃N@C₈₆, the cluster undergoes nearly free isotropic rotation.[29] Moreover, a comprehensive ¹⁴N NMR study on A₃N@C₈₀ (A = Sc, Y, or Lu) was reported by Dorn et al., suggesting that the rotation energetic barriers of the clusters are dependent on the ionic radius of the metal ions.[38]

Over the last 10−12 years, the structural characterization of TNT-EMFs has been supported by several seminal computational studies. For example, early computational results by Nagase supported significant charge transfer of approximately six electrons to the icosahedral I_h-C₈₀ cage, and predicted a relatively large (6.5 eV) band gap in archetypal Sc₃N@I_h-C₈₀.[8] Aihara predicted exceptional stability for the I_h-C₈₀ cage based on a Hückel minimum bond resonance energies (min BRE) approach.[39] More recently, Poblet and co-workers have advanced a rule based on a simple ionic model for transfer of six electrons from the trimetallic nitride cluster for Sc₃N@D_3-C₆₈, Sc₃N@D_{3h}-C₇₈, and Sc₃N@I_h-C₈₀.[12,40] This rule predicts that a suitable fullerene must
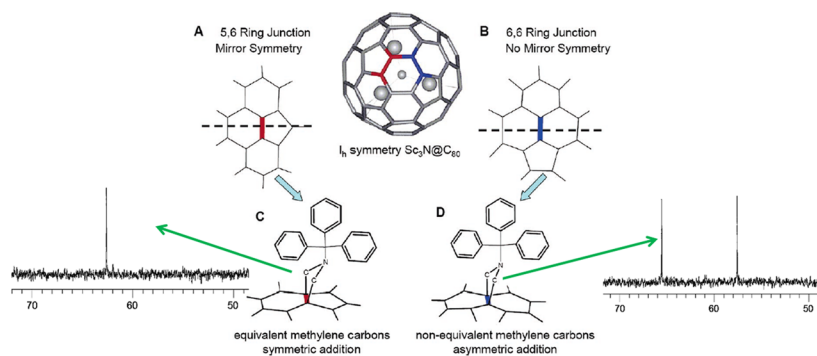
FIGURE 7. The ^{13}C NMR spectral differences between the [6,6] and [5,6] 1,3-dipolar derivatives of Sc$_3$N@C$_{80}$.

host three low-lying unoccupied molecular orbitals and there must be sizable gap between the LUMO-4 and LUMO-3 orbitals where LUMO-n is the nth-lowest unoccupied MO. A very detailed DFT study by Popov and Dunsch has shown that, for the isomers of A$_3$N@C$_{2n}$ (A = Sc and Y, $2n = 68-98$), based on the most stable C$_{2n}^{6-}$, the lowest energy isomers for Sc$_3$N@C$_{68}$, Sc$_3$N@C$_{78}$, Sc$_3$N@C$_{80}$, Y$_3$N@C$_{80}$, Y$_3$N@C$_{84}$, Y$_3$N@C$_{86}$, and Y$_3$N@C$_{88}$ are the same ones found from the single-crystal X-ray studies, *vide supra*.[41]

5. Cage Surface Functionalization Reactions of TNT-EMFs

The hydrophobic cage surface of the TNT-EMFs requires chemical functionalization as a prerequisite for many potential applications. As noted in section 3, the TNT-EMFs are more reactive toward Lewis acids (AlCl$_3$) but are less reactive toward nucleophilic amines (Lewis bases), in comparison with empty-cage fullerenes (C$_{60}$, C$_{70}$, and C$_{84}$). The first reported derivative of a TNT-EMF was an isochromanone Diels−Alder adduct of Sc$_3$N@I_h-C$_{80}$,[42] which was characterized by ^{13}C NMR. Subsequently, a single-crystal X-ray crystallographic structure was obtained by Balch's laboratory.[43] The Diels−Alder addition reaction also provided the first derivative of the promising candidate for the next-generation MRI contrast agent, Gd$_3$N@C$_{80}$, *vide infra*.[44] Echegoyen and co-workers reported a 1,3-dipolar cycloaddition reaction of *N*-ethylazomethine ylide yielded mainly the pyrrolidine monoadduct of TNT-EMFs. They found that the cycloaddition reaction occurred across the [6,6] bond for Y$_3$N@I_h-C$_{80}$, but the [5,6] addition occurred for Sc$_3$N@I_h-C$_{80}$.[45] Later, the Dorn laboratory reported that both [5,6] and [6,6] addition occur for the case of *N*-tritylpyrrolidino derivatives of Sc$_3$N@I_h-C$_{80}$.[46] The kinetically favored [6,6] *N*-tritylpyrrolidino derivative is initially formed in greater abundance, while the thermodynamically favored [5,6] isomer

predominates at longer reaction times. As illustrated in Figure 7, the [5,6] *N*-tritylpyrrolidino isomer yields symmetric methylene groups and exhibits only one signal between 50 and 70 ppm in ^{13}C NMR spectrum, in contrast with the [6,6] addition isomer, which exhibits two signals. Interconversion of isomers was confirmed by heating the kinetically favored [6,6] product and following the conversion to the [5,6] isomer. Interestingly, Chen et al. investigated the influence of cluster size on the reaction sites for the Sc$_x$Gd$_{3-x}$N@C$_{80}$ ($x = 0-3$) series with a similar 1,3-dipolar cycloaddition reaction.[47] They found that the larger (Gd$_3$N)$^{6+}$ cluster led to a preponderance of the [6,6] derivative for Gd$_3$N@C$_{80}$ while the [5,6] product dominated in the smaller (ScGd$_2$N)$^{6+}$ and (Sc$_2$GdN)$^{6+}$ clusters.

The Bingel 1,3-cycloaddition reaction also gives a series of important TNT-EMF derivatives, among them the important open-cage Bingel derivative of Y$_3$N@I_h-C$_{80}$ occurring via bromomalonate addition.[48] Echegoyen and co-workers found that one yttrium atom (Y$_1$) was fixed near the open site of this adduct, while the other two yttrium atoms (Y$_2$ and Y$_3$) could rotate about the Y$_1$−N axis of the (Y$_3$N)$^{6+}$ cluster. Although it was earlier reported that Sc$_3$N@I_h-C$_{80}$ was unreactive in the usual Bingel reaction conditions,[45] the Dorn laboratory synthesized a cyclopropanyl adduct of Sc$_3$N@I_h-C$_{80}$ with catalytic manganese(III) via a radical mechanism.[49] Alternatively, the Echegoyen laboratory has shown that, in the presence of DMF, Sc$_3$N@I_h-C$_{80}$ can also react with bromomalonate to form Bingel adducts in a similar fashion to the Y$_3$N@I_h-C$_{80}$.[50] A 1,3-dipolar addition diazo reaction has been reported, yielding phenyl-A$_3$NC$_{81}$-butyric methylate (A = Lu, Sc, or Y) TNT-EMF derivatives, which are important new materials as electron acceptors for heterojunction photovoltaic solar cell devices.[51,52] Echegoyen and co-workers[53] have also reported the interesting [2 + 2] reaction of isoamyl nitrite and anthranilic acid with Sc$_3$N@I_h-C$_{80}$, which leads to a benzyne intermediate followed by formation
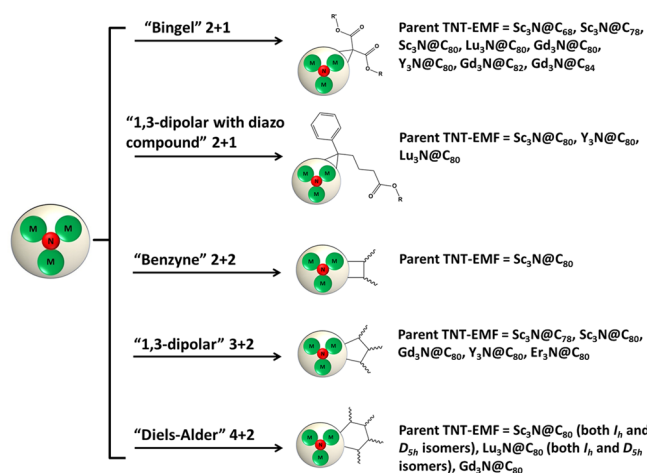
FIGURE 8. Major types of cycloaddition reactions developed on TNT-EMFs.

of monoadducts with a four-membered ring attached to the cage surface via both [5,6] and [6,6] ring addition.

A minor C_{80} isomer of the TNT-EMF family, $A_3N@D_{5h}$-C_{80} (A = Sc or Lu), was found to exhibit enhanced chemical reactivity in both the Diels—Alder and 1,3-dipolar reactions (Figure 8), in comparison with the I_h isomer.[54] The two 1,3-dipolar addition products for $A_3N@D_{5h}$-C_{80} were assigned by ^{1}H NMR, but an alternative assignment has been advanced for one of these products in a recent computational report.[55] The smaller TNT-EMF, $Sc_3N@D_{3h}$-C_{78}, was also functionalized with both the 1,3-dipolar reaction[56] and the Bingel reaction,[57] in which both mono- and bis-adduct were isolated and characterized. Some non-IPR TNT-EMFs, including $Sc_3N@D_3$-C_{68}, $Gd_3N@C_s$-C_{82}, and $Gd_3N@C_s$-C_{84}, are also reactive toward the Bingel reaction;[58−60] the structural characterization of TNT-EMF derivatives is largely limited to computational results.

Trifluoromethylation radical reactions of TNT-EMFs via a radical mechanism have been conducted on $Sc_3N@C_{80}$ (both I_h and D_{5h} isomers), yielding $Sc_3N@C_{80}(CF_3)_{2n}$ ($n = 1$–6)[61] products. Another UV-initiated radical reaction between benzyl bromide and $Sc_3N@I_h$-C_{80} yields exclusively $Sc_3N@C_{80}(C_7H_8)_2$.[62] In both trifluoromethylation and benzyl radical reactions, the functional groups are added pairwise with 1,4 addition across the hexagon rings (para addition) on the fullerene surface. The TNT-EMFs have also been functionalized by multiaddition hydroxylation and carboxylation reactions for MRI contrast agents[63] and electrochemical approaches.[64,65] Very recently (during preparation of this Account), Akasaka and co-workers reported an interesting monosilylation reaction of $Lu_3N@C_{80}$.[66] Other important chemical functionalization reactions not detailed in this review are discussed in more comprehensive reviews.[11,13]

6. Applications of TNT-EMFs

It is well recognized that there are several potential applications for the TNT-EMFs. For biomedical applications, the TNT-EMF cage has the inherent advantage of high stability and characteristic resistance to any potential biological metabolic cage-opening process(es), which enables the application of toxic lanthanide ions without the risk of their release to surrounding biological components. On the other hand, the lower chemical reactivity of the $A_3N@C_{2n}$ family, *vide supra*, is still sufficient for functionalization by a variety of reactions to convert the hydrophobic fullerene surface to a hydrophilic water/biological fluid-compatible surface for drug delivery.

A seminal study by Shinohara et al. demonstrated that the hydroxylated metallofullerene, $Gd@C_{82}(OH)_n$, exhibits excellent characteristics as an MRI contrast agent, with relaxivity at several different magnetic field strengths (r_1 up to 81 mM^{-1} s^{-1}, 10−20 times higher than commercial MRI contrast agents Omniscan and Magnevist).[67] Since 2006, several *in vitro* and *in vivo* MRI relaxivity studies of TNT-EMF $Gd_3N@C_{80}$ derivatives have been reported and reviewed. For example, water-soluble poly(ethylene glycol) functionalized and hydroxylated TNT-EMF derivatives, $Gd_3N@C_{80}[DiPEG(OH)_x]$,[68] were found to have the highest reported relaxivities, with values of 237 mM^{-1} s^{-1} for r_1 and 460 mM^{-1} s^{-1} for r_2 (79 mM^{-1} s^{-1} and 153 mM^{-1} s^{-1} based on Gd^{3+} ion) at a clinical-range magnetic field of 2.4 T.[69] The Dorn laboratory and collaborators from Virginia Commonwealth University have reported a TNT-EMF nanoplatform with ^{177}Lu brachytherapy in a murine glioblastoma multiforme (GBM) model that increases median survival from 21 to 52 days with long-term diagnostic MRI.[70] More recently, this collaborative group has reported even longer median survival to over 120 days with a multimodal "theranostic" radiolabeled ^{177}Lu-DOTA-f-$Gd_3N@C_{80}$ EMF platform (Figure 9).[71] In both of these studies, the approach involves external functionalization chemistry and subsequent treatment with a radiolabeled [177]LuCl$_3$ sample. In contrast to exohedral radiolanthanide EMFs, the encapsulation of radionuclide atoms or clusters inside fullerene cages provides a nearly ideal platform, since the radioactive metal ion is completely isolated from the biosystem. We described the preparation of the [177]Lu$_x$Lu$_{(3−x)}$N@C_{80}−TAMRA−IL-13 peptide[72] using a remotely-controlled K−H generator to prepare the ^{177}Lu in a TNT-EMF cage, and demonstrated that, for a period of at least one half-life (6.7 days), the encapsulated [177]Lu^{3+} ions are not released. This [177]Lu
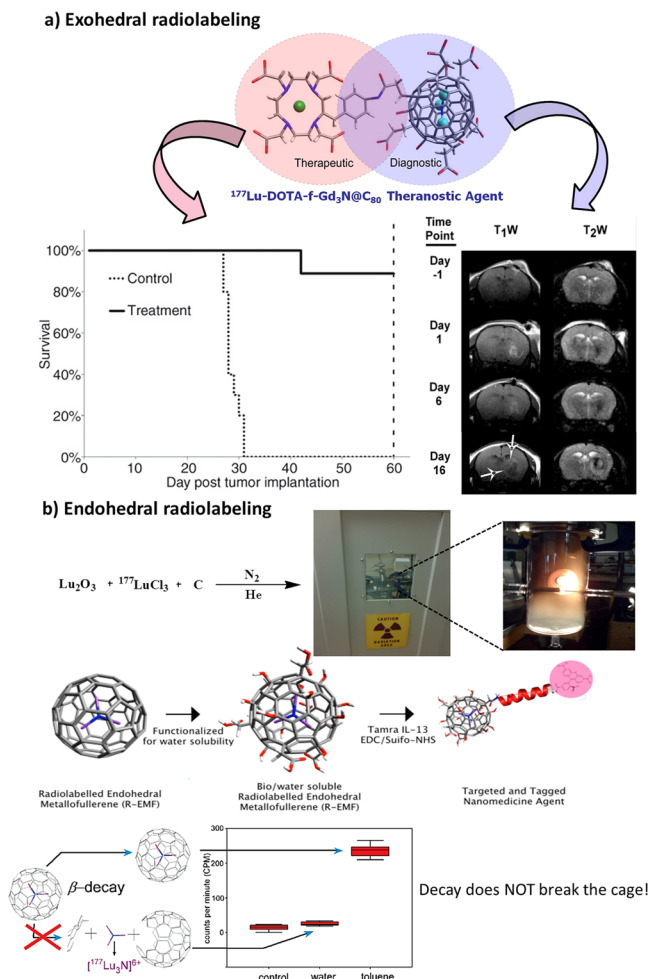
FIGURE 9. Exohedral and endohedral radiolabeling of TNT-EMF derivatives.

radiolabeled EMF agent was subsequently conjugated with a fluorescence tag (TAMRA) and interleukin-13 (IL-13), a cytokine peptide designed to target overexpressed receptor cells in GBM. Of critical importance for biomedical applications, a recent study reported no notable cytotoxicity for primary mouse brain neuronal cells and human neuroblastoma cells treated with functionalized TNT-EMFs and empty-cage fullerenes in concentrations up to 10 μM.[73]

TNT-EMFs have also emerged as promising building blocks for various semiconductor, optoelectronic, and light electron/energy conversion systems. As one example, metallofullerenes are among leading candidates for electron acceptors in organic photovoltaic devices. In 2009, Ross and colleagues demonstrated the importance of TNT-EMFs in this field with the derivative phenyl-$Lu_3N@C_{81}$ butyric hexyl ester (also known as $Lu_3N@C_{80}$–PCBH), which exhibits one of the highest open circuit voltages ($V_{OC} = 810$ mV) reported to date, and an improved efficiency (4.2%) directly compared with the corresponding C_{60}PCBM derivative under the same condition ($V_{OC} = 630$ mV, 3.4% efficiency).[51] On the other

hand, the short circuit current of this system is lower than the C_{60}PCBM, and the reason was recently investigated.[74] In a paradigm shift, the TNT-EMF was shown to exhibit not only electron acceptor properties but also electron donation in a covalently linked $Lu_3N@C_{80}$–perylenediimide (PDI) conjugate, in which PDI acts as the light harvester and the electron acceptor.[75] Also of note, Novotny has coupled single $Y_3N@C_{80}$ molecules to single gold nanoparticles as optical antennas to drastically enhance light absorption and emission from poor emitters like rare-earth ions.[76] Although it has been over 13 years since the discovery of the TNT-EMFs, their applications (especially as MRI contrast agents and photovoltaic electron acceptors) are only starting to mature. Recent commercial availability of TNT-EMFs should change this situation over the next several years.

BIOGRAPHICAL INFORMATION

Jianyuan Zhang joined the Dorn group for his Ph.D. study after graduation from Beijing Normal University. His research includes characterization and functionalization of metallofullerenes.

Steven Stevenson received his Ph.D. for metallofullerene research at Virginia Tech in 1995. After a hiatus, he returned to VT as a Research Scientist/Visiting Professor (1997−2000) where he taught Chemistry and performed research with Harry Dorn. During this time, Stevenson and Dorn discovered the trimetallic nitride template (TNT) molecules. Prof. Stevenson is currently at Indiana University−Purdue University at Fort Wayne working on another new class of molecules (metallic oxide clusters in fullerene cages).

Harry C. Dorn received his Ph.D, from University of California, Davis, in 1974, and joined the faculty of Chemistry at Virginia Tech the same year. In 2010, he was named A.C. Lilly, Jr., Faculty Fellow of Nanoscience. In 2012, he became dual-title professor at the Virginia Tech Carilion Research Institute and professor of Chemistry in the College of Science at Virginia Tech. His research interests include electron and nuclear resonance phenomena (NMR, EPR, and DNP), as well as new forms of carbonaceous nanomaterials, including fullerenes, metallofullerenes, nanotubes, and nanohorns.

FOOTNOTES

*To whom correspondence should be addressed. E-mail addresses: stevenss@ipfw.edu; hdorn@vt.edu.
The authors declare no competing financial interest.

REFERENCES

1 Kroto, H. W.; Heath, J. R.; Obrien, S. C.; Curl, R. F.; Smalley, R. E. C_{60}-buckministerfullerene. *Nature* **1985**, *318*, 162–163.

2 Yamada, M.; Akasaka, T.; Nagase, S. Endohedral metal atoms in pristine and functionalized fullerene cages. *Acc. Chem. Res.* **2010**, *43*, 92–102.

3 Kratschmer, W.; Fostiropoulos, K.; Huffman, D. R. The infrared and ultraviolet-absorption spectra of laboratory-produced carbon dust-evidence for the prescence of the C_{60} molecule. *Chem. Phys. Lett.* **1990**, *170*, 167–170.

4 Stevenson, S.; Dorn, H. C.; Burbank, P.; Harich, K.; Haynes, J.; Kiang, C. H.; Salem, J. R.; Devries, M. S.; Vanloosdrecht, P. H. M.; Johnson, R. D.; Yannoni, C. S.; Bethune, D. S. Automated HPLC separation of endohedral metallofullerene $Sc@C_{2n}$ and $Y@C_{2n}$ fractions. *Anal. Chem.* **1994**, *66*, 2675–2679.

5 Yeretzian, C.; Hansen, K.; Alvarez, M. M.; Min, K. S.; Gillan, E. G.; Holczer, K.; Kaner, R. B.; Whetten, R. L. Collisional probes and possible structures of $La@C_{80}$. *Chem. Phys. Lett.* **1992**, *196*, 337–342.

6 Akasaka, T.; Nagase, S.; Kobayashi, K.; Wälchli, M.; Yamamoto, K.; Funasaka, H.; Kako, M.; Hoshino, T.; Erata, T. ^{13}C and ^{139}La NMR studies of $La_2@C_{80}$: First evidence for circular motion of metal atoms in endohedral dimetallofullerenes. *Angew. Chem., Int. Ed.* **1997**, *36*, 1643–1645.

7 Stevenson, S.; Rice, G.; Glass, T.; Harich, K.; Cromer, F.; Jordan, M. R.; Craft, J.; Hadju, E.; Bible, R.; Olmstead, M. M.; Maitra, K.; Fisher, A. J.; Balch, A. L.; Dorn, H. C. Small-bandgap endohedral metallofullerenes in high yield and purity. *Nature* **1999**, *401*, 55–57.

8 Kobayashi, K.; Sano, Y.; Nagase, S. Theoretical study of endohedral metallofullerenes: $Sc_{3-n}La_nN@C80$ (n=0—3). *J. Comput. Chem.* **2001**, *22*, 1353–1358.

9 Dunsch, L.; Yang, S. Metal nitride cluster fullerenes: Their current state and future prospects. *Small* **2007**, *3*, 1298–1320.

10 Lu, X.; Akasaka, T.; Nagase, S. Chemistry of endohedral metallofullerenes: The role of metals. *Chem. Commun.* **2011**, *47*, 5942–5957.

11 Chaur, M. N.; Melin, F.; Ortiz, A. L.; Echegoyen, L. Chemical, electrochemical, and structural properties of endohedral metallofullerenes. *Angew. Chem., Int. Ed.* **2009**, *48*, 7514–7538.

12 Rodriguez-Fortea, A.; Balch, A. L.; Poblet, J. M. Endohedral metallofullerenes: A unique host-guest association. *Chem. Soc. Rev.* **2011**, *40*, 3551–3563.

13 Lu, X.; Feng, L.; Akasaka, T.; Nagase, S. Current status and future developments of endohedral metallofullerenes. *Chem. Soc. Rev.* **2012**, *41*, 7723–7760.

14 Dunsch, L.; Krause, M.; Noack, J.; Georgi, P. Endohedral nitride cluster fullerenes: Formation and spectroscopic analysis of $L_{3-x}M_xN@C_{2n}$ ($0 \leq x \leq 3$; N=39,40). *J. Phys. Chem. Solids* **2004**, *65*, 309–315.

15 Stevenson, S.; Thompson, M. C.; Coumbe, H. L.; Mackey, M. A.; Coumbe, C. E.; Phillips, J. P. Chemically adjusting plasma temperature, energy, and reactivity (CAPTEAR) method using NO_x and combustion for selective synthesis of $Sc_3N@C_{80}$ metallic nitride fullerenes. *J. Am. Chem. Soc.* **2007**, *129*, 16257–16262.

16 Stevenson, S.; Mackey, M. A.; Thompson, M. C.; Coumbe, H. L.; Madasu, P. K.; Coumbe, C. E.; Phillips, J. P. Effect of copper metal on the yield of $Sc_3N@C_{80}$ metallofullerenes. *Chem. Commun.* **2007**, 4263–4265.

17 Ling, Y.; Stevenson, S.; Zhang, Y. Metallic nitride azafullerenes: A novel class of fullerenes with interesting electronic properties. *Chem. Phys. Lett.* **2011**, *508*, 121–124.

18 Ge, Z. X.; Duchamp, J. C.; Cai, T.; Gibson, H. W.; Dorn, H. C. Purification of endohedral trimetallic nitride fullerenes in a single, facile step. *J. Am. Chem. Soc.* **2005**, *127*, 16292–16298.

19 Stevenson, S.; Harich, K.; Yu, H.; Stephen, R. R.; Heaps, D.; Coumbe, C.; Phillips, J. P. Nonchromatographic "stir and filter approach" (SAFA) for isolating $Sc_3N@C_{80}$ metallofullerenes. *J. Am. Chem. Soc.* **2006**, *128*, 8829–8835.

20 Stevenson, S.; Mackey, M. A.; Coumbe, C. E.; Phillips, J. P.; Elliott, B.; Echegoyen, L. Rapid removal of D_{5h} isomer using the "stir and filter approach" and isolation of large quantities of isomerically pure $Sc_3N@C_{80}$ metallic nitride fullerenes. *J. Am. Chem. Soc.* **2007**, *129*, 6072–6073.

21 Angeli, C. D.; Cai, T.; Duchamp, J. C.; Reid, J. E.; Singer, E. S.; Gibson, H. W.; Dorn, H. C. Purification of trimetallic nitride templated endohedral metallofullerenes by a chemical reaction of congeners with eutectic 9-methylanthracene. *Chem. Mater.* **2008**, *20*, 4993–4997.

22 Stevenson, S.; Mackey, M. A.; Pickens, J. E.; Stuart, M. A.; Confait, B. S.; Phillips, J. P. Selective complexation and reactivity of metallic nitride and oxometallic fullerenes with Lewis acids and use as an effective purification method. *Inorg. Chem.* **2009**, *48*, 11685–11690.

23 Stevenson, S.; Phillips, J. P.; Reid, J. E.; Olmstead, M. M.; Rath, S. P.; Balch, A. L. Pyramidalization of Gd_3N inside a C_{80} cage. The synthesis and structure of $Gd_3N@C_{80}$. *Chem. Commun.* **2004**, 2814–2815.

24 Olmstead, M. H.; de Bettencourt-Dias, A.; Duchamp, J. C.; Stevenson, S.; Marciu, D.; Dorn, H. C.; Balch, A. L. Isolation and structural characterization of the endohedral fullerene $Sc_3N@C_{78}$. *Angew. Chem., Int. Ed.* **2001**, *40*, 1223–1225.

25 Popov, A. A.; Krause, M.; Yang, S.; Wong, J.; Dunsch, L. C_{78} cage isomerism defined by trimetallic nitride cluster size: A computational and vibrational spectroscopic study. *J. Phys. Chem. B* **2007**, *111*, 3363–3369.

26 Beavers, C. M.; Chaur, M. N.; Olmstead, M. M.; Echegoyen, L.; Balch, A. L. Large metal ions in a relatively small fullerene cage: The structure of $Gd_3N@C_2(22010)C_{78}$ departs from the isolated pentagon rule. *J. Am. Chem. Soc.* **2009**, *131*, 11519–11524.

27 Ma, Y.; Wang, T.; Wu, J.; Feng, Y.; Xu, W.; Jiang, L.; Zheng, J.; Shu, C.; Wang, C. Size effect of endohedral cluster on fullerene cage: Preparation and structural studies of $Y_3N@C_{78}$-C_2. *Nanoscale* **2011**, *3*, 4955–4957.

28 Mercado, B. Q.; Beavers, C. M.; Olmstead, M. M.; Chaur, M. N.; Walker, K.; Holloway, B. C.; Echegoyen, L.; Balch, A. L. Is the isolated pentagon rule merely a suggestion for endohedral fullerenes? The structure of a second egg-shaped endohedral fullerene—$Gd_3N@C_s(39663)$-C_{82}. *J. Am. Chem. Soc.* **2008**, *130*, 7854–7855.

29 Fu, W.; Xu, L.; Azurmendi, H.; Ge, J.; Fuhrer, T.; Zuo, T.; Reid, J.; Shu, C.; Harich, K.; Dorn, H. C. ^{89}Y and ^{13}C NMR cluster and carbon cage studies of an yttrium metallofullerene family, $Y_3N@C_{2n}$ (n = 40—43). *J. Am. Chem. Soc.* **2009**, *131*, 11762–11769.

30 Beavers, C. M.; Zuo, T.; Duchamp, J. C.; Harich, K.; Dorn, H. C.; Olmstead, M. M.; Balch, A. L. $Tb_3N@C_{84}$: An improbable, egg-shaped endohedral fullerene that violates the isolated pentagon rule. *J. Am. Chem. Soc.* **2006**, *128*, 11352–11353.

31 Zuo, T.; Walker, K.; Olmstead, M. M.; Melin, F.; Holloway, B. C.; Echegoyen, L.; Dorn, H. C.; Chaur, M. N.; Chancellor, C. J.; Beavers, C. M.; Balch, A. L.; Athans, A. J. New egg-shaped fullerenes: Non-isolated pentagon structures of $Tm_3N@C_s(51365)$-C_{84} and $Gd_3N@C_s(51365)$-C_{84}. *Chem. Commun.* **2008**, 1067–1069.

32 Zuo, T.; Beavers, C. M.; Duchamp, J. C.; Campbell, A.; Dorn, H. C.; Olmstead, M. M.; Balch, A. L. Isolation and structural characterization of a family of endohedral fullerenes including the large, chiral cage fullerenes $Tb_3N@C_{88}$ and $Tb_3N@C_{86}$ as well as the I_h and D_{5h} isomers of $Tb_3N@C_{80}$. *J. Am. Chem. Soc.* **2007**, *129*, 2035–2043.

33 Chaur, M. N.; Aparicio-Angles, X.; Mercado, B. Q.; Elliott, B.; Rodriguez-Fortea, A.; Clotet, A.; Olmstead, M. M.; Balch, A. L.; Poblet, J. M.; Echegoyen, L. Structural and electrochemical property correlations of metallic nitride endohedral metallofullerenes. *J. Phys. Chem. C* **2010**, *114*, 13003–13009.

34 Fu, W.; Zhang, J.; Champion, H.; Fuhrer, T.; Azuremendi, H.; Zuo, T.; Zhang, J.; Harich, K.; Dorn, H. C. Electronic properties and ^{13}C NMR structural study of $Y_3N@C_{88}$. *Inorg. Chem.* **2011**, *50*, 4256–4259.

35 Stevenson, S.; Fowler, P. W.; Heine, T.; Duchamp, J. C.; Rice, G.; Glass, T.; Harich, K.; Hajdu, E.; Bible, R.; Dorn, H. C. A stable non-classical metallofullerene family. *Nature* **2000**, *408*, 427–428.

36 Chaur, M. N.; Melin, F.; Ashby, J.; Elliott, B.; Kumbhar, A.; Rao, A. M.; Echegoyen, L. Lanthanum nitride endohedral fullerenes $La_3N@C_{2n}$ ($43 \leq n \leq 55$): Preferential formation of $La_3N@C_{96}$. *Chem.—Eur. J.* **2008**, *14*, 8213–8219.

37 Olmstead, M. M.; Lee, H. M.; Duchamp, J. C.; Stevenson, S.; Marciu, D.; Dorn, H. C.; Balch, A. L. $Sc_3N@C_{68}$: Folded pentalene coordination in an endohedral fullerene that does not obey the isolated pentagon rule. *Angew. Chem., Int. Ed.* **2003**, *42*, 900–903.

38 Fu, W.; Wang, X.; Azuremendi, H.; Zhang, J.; Dorn, H. C. N-14 and Sc-45 NMR study of trimetallic nitride cluster $(M_3N)^{6+}$ dynamics inside an icosahedral C_{80} cage. *Chem. Commun.* **2011**, *47*, 3858–3860.

39 Aihara, J. Kinetic stability of metallofullerenes as predicted by the bond resonance energy model. *Phys. Chem. Chem. Phys.* **2001**, *3*, 1427–1431.

40 Rodriguez-Fortea, A.; Alegret, N.; Balch, A. L.; Poblet, J. M. The maximum pentagon separation rule provides a guideline for the structures of endohedral metallofullerenes. *Nat. Chem.* **2010**, *2*, 955–961.

41 Popov, A. A.; Dunsch, L. Structure, stability, and cluster-cage interactions in nitride clusterfullerenes $M_3N@C_{2n}$ (M = Sc, Y; 2n = 68—98): A density functional theory study. *J. Am. Chem. Soc.* **2007**, *129*, 11835–11849.

42 Iezzi, E. B.; Duchamp, J. C.; Harich, K.; Glass, T. E.; Lee, H. M.; Olmstead, M. M.; Balch, A. L.; Dorn, H. C. A symmetric derivative of the trimetallic nitride endohedral metallofullerene, $Sc_3N@C_{80}$. *J. Am. Chem. Soc.* **2002**, *124*, 524–525.

43 Lee, H. M.; Olmstead, M. M.; Iezzi, E.; Duchamp, J. C.; Dorn, H. C.; Balch, A. L. Crystallographic characterization and structural analysis of the first organic functionalization product of the endohedral fullerene $Sc_3N@C_{80}$. *J. Am. Chem. Soc.* **2002**, *124*, 3494–3495.

44 Stevenson, S.; Stephen, R. R.; Amos, T. M.; Cadorette, V. R.; Reid, J. E.; Phillips, J. P. Synthesis and purification of a metallic nitride fullerene bisAdduct: Exploring the reactivity of $Gd_3N@C_{80}$. *J. Am. Chem. Soc.* **2005**, *127*, 12776–12777.

45 Cardona, C. M.; Kitaygorodskiy, A.; Echegoyen, L. Trimetallic nitride endohedral metallofullerenes: Reactivity dictated by the encapsulated metal cluster. *J. Am. Chem. Soc.* **2005**, *127*, 10448–10453.

46 Cai, T.; Slebodnick, C.; Xu, L.; Harich, K.; Glass, T. E.; Chancellor, C.; Fettinger, J. C.; Olmstead, M. M.; Balch, A. L.; Gibson, H. W.; Dorn, H. C. A pirouette on a metallofullerene sphere: interconversion of isomers of N-tritylpyrrolidino I_h $Sc_3N@C_{80}$. *J. Am. Chem. Soc.* **2006**, *128*, 6486–6492.

47 Chen, N.; Zhang, E.; Tan, K.; Wang, C.; Lu, X. Size effect of encaged clusters on the exohedral chemistry of endohedral fullerenes: A case study on the pyrrolidino reaction of $Sc_xGd_{3-x}N@C_{80}$ (x = 0—3). *Org. Lett.* **2007**, *9*, 2011–2013.

48 Lukoyanova, O.; Cardona, C. M.; Rivera, J.; Lugo-Morales, L. Z.; Chancellor, C. J.; Olmstead, M. M.; Rodriguez-Fortea, A.; Poblet, J. M.; Balch, A. L.; Echegoyen, L. "Open rather than closed" malonate methano-fullerene derivatives. The formation of methanofulleroid adducts of $Y_3N@C_{80}$. *J. Am. Chem. Soc.* **2007**, *129*, 10423–10430.

49 Shu, C.; Cai, T.; Xu, L.; Zuo, T.; Reid, J.; Harich, K.; Dorn, H. C.; Gibson, H. W. Manganese(III)-catalyzed free radical reactions on trimetallic nitride endohedral metallofullerenes. *J. Am. Chem. Soc.* **2007**, *129*, 15710–15717.

50 Pinzon, J. R.; Zuo, T.; Echegoyen, L. Synthesis and electrochemical studies of Bingel-Hirsch derivatives of $M_3N@I_h-C_{80}$ (M = Sc, Lu). *Chem.—Eur. J.* **2010**, *16*, 4864–4869.

51 Ross, R. B.; Cardona, C. M.; Guldi, D. M.; Sankaranarayanan, S. G.; Reese, M. O.; Kopidakis, N.; Peet, J.; Walker, B.; Bazan, G. C.; Van Keuren, E.; Holloway, B. C.; Drees, M. Endohedral fullerenes for organic photovoltaic devices. *Nat. Mater.* **2009**, *8*, 208–212.

52 Shu, C.; Xu, W.; Slebodnick, C.; Champion, H.; Fu, W.; Reid, J. E.; Azurmendi, H.; Wang, C.; Harich, K.; Dorn, H. C.; Gibson, H. W. Syntheses and structures of phenyl-C_{81}-butyric acid methyl esters (PCBMs) from $M_3N@C_{80}$. *Org. Lett.* **2009**, *11*, 1753–1756.

53 Li, F.-F.; Pinzon, J. R.; Mercado, B. Q.; Olmstead, M. M.; Balch, A. L.; Echegoyen, L. 2 + 2 Cycloaddition Reaction to $Sc_3N@I_h-C_{80}$. The Formation of very stable 5,6- and 6,6-adducts. *J. Am. Chem. Soc.* **2011**, *133*, 1563–1571.

54 Cai, T.; Xu, L.; Anderson, M. R.; Ge, Z.; Zuo, T.; Wang, X.; Olmstead, M. M.; Balch, A. L.; Gibson, H. W.; Dorn, H. C. Structure and enhanced reactivity rates of the D_{5h} $Sc_3N@C_{80}$ and $Lu_3N@C_{80}$ metallofullerene isomers: the importance of the pyracylene motif. *J. Am. Chem. Soc.* **2006**, *128*, 8581–8589.

55 Osuna, S.; Rodriguez-Fortea, A.; Poblet, J. M.; Sola, M.; Swart, M. Product formation in the Prato reaction on $Sc_3N@D_{5h}-C_{80}$: Preference for [5,6]-bonds, and not pyracylenic bonds. *Chem.Commun.* **2012**, *48*, 2486–2488.

56 Cai, T.; Xu, L.; Gibson, H. W.; Dorn, H. C.; Chancellor, C. J.; Olmstead, M. M.; Balch, A. L. $Sc_3N@C_{78}$: Encapsulated cluster regiocontrol of adduct docking on an ellipsoidal metallofullerene sphere. *J. Am. Chem. Soc.* **2007**, *129*, 10795–10800.

57 Cai, T.; Xu, L.; Shu, C.; Champion, H. A.; Reid, J. E.; Anklin, C.; Anderson, M. R.; Gibson, H. W.; Dorn, H. C. Selective formation of a symmetric $Sc_3N@C_{78}$ bisadduct: adduct docking controlled by an internal trimetallic nitride cluster. *J. Am. Chem. Soc.* **2008**, *130*, 2136–2137.

58 Cai, T.; Xu, L.; Shu, C.; Reid, J. E.; Gibson, H. W.; Dorn, H. C. Synthesis and characterization of a non-IPR fullerene derivative: $Sc_3N@C_{68}C(COOC_2H_5)_2$. *J. Phys. Chem. C* **2008**, *112*, 19203–19208.

59 Chaur, M. N.; Melin, F.; Athans, A. J.; Elliott, B.; Walker, K.; Holloway, B. C.; Echegoyen, L. The influence of cage size on the reactivity of trimetallic nitride metallofullerenes: a mono- and bis-methanoadduct of $Gd_3N@C_{80}$ and a monoadduct of $Gd_3N@C_{84}$. *Chem. Commun.* **2008**, 2665–2667.

60 Alegret, N.; Chaur, M. N.; Santos, E.; Rodriguez-Fortea, A.; Echegoyen, L.; Poblet, J. M. Bingel—Hirsch reactions on non-IPR $Gd_3N@C_{2n}$ (2n = 82 and 84). *J. Org. Chem.* **2010**, *75*, 8299–8302.

61 Shustova, N. B.; Popov, A. A.; Mackey, M. A.; Coumbe, C. E.; Phillips, J. P.; Stevenson, S.; Strauss, S. H.; Boltalina, O. V. Radical trifluoromethylation of $Sc_3N@C_{80}$. *J. Am. Chem. Soc.* **2007**, *129*, 11676–11677.

62 Shu, C.; Slebodnick, C.; Xu, L.; Champion, H.; Fuhrer, T.; Cai, T.; Reid, J. E.; Fu, W.; Harich, K.; Dorn, H. C.; Gibson, H. W. Highly regioselective derivatization of trimetallic nitride templated endohedral metallofullerenes via a facile photochemical reaction. *J. Am. Chem. Soc.* **2008**, *130*, 17755–17760.

63 Shu, C.; Corwin, F. D.; Zhang, J.; Chen, Z.; Reid, J. E.; Sun, M.; Xu, W.; Sim, J. H.; Wang, C.; Fatouros, P. P.; Esker, A. R.; Gibson, H. W.; Dorn, H. C. Facile preparation of a new

64 Li, F.-F.; Rodríguez-Fortea, A.; Poblet, J. M.; Echegoyen, L. Reactivity of metallic nitride endohedral metallofullerene anions: electrochemical synthesis of a $Lu_3N@I_h-C_{80}$ derivative. *J. Am. Chem. Soc.* **2011**, *133*, 2760–2765.

65 Li, F.-F.; Rodríguez-Fortea, A.; Peng, P.; Campos Chavez, G. A.; Poblet, J. M.; Echegoyen, L. Electrosynthesis of a $Sc_3N@I_h-C_{80}$ methano derivative from trianionic $Sc_3N@I_h-C_{80}$. *J. Am. Chem. Soc.* **2012**, *134*, 7480–7487.

66 Sato, K.; Kako, M.; Suzuki, M.; Mizorogi, N.; Tsuchiya, T.; Olmstead, M. M.; Balch, A. L.; Akasaka, T.; Nagase, S. Synthesis of silylene-bridged endohedral metallofullerene $Lu_3N@I_h-C_{80}$. *J. Am. Chem. Soc.* **2012**, *134*, 16033–16039.

67 Mikawa, M.; Kato, H.; Okumura, M.; Narazaki, M.; Kanazawa, Y.; Miwa, N.; Shinohara, H. Paramagnetic water-soluble metallofullerenes having the highest relaxivity for MRI contrast agents. *Bioconjugate Chem.* **2001**, *12*, 510–514.

68 Fatouros, P. P.; Corwin, F. D.; Chen, Z.-J.; Broaddus, W. C.; Tatum, J. L.; Kettenmann, B.; Ge, Z.; Gibson, H. W.; Russ, J. L.; Leonard, A. P.; Duchamp, J. C.; Dorn, H. C. In vitro and in vivo imaging studies of a new endohedral metallofullerene nanoparticle. *Radiology* **2006**, *240*, 756–764.

69 Zhang, J.; Fatouros, P. P.; Shu, C.; Reid, J.; Owens, L. S.; Cai, T.; Gibson, H. W.; Long, G. L.; Corwin, F. D.; Chen, Z.-J.; Dorn, H. C. High relaxivity trimetallic nitride (Gd_3N) metallofullerene MRI contrast agents with optimized functionality. *Bioconjugate Chem.* **2010**, *21*, 610–615.

70 Fillmore, H. L.; Shultz, M. D.; Henderson, S. C.; Cooper, P.; Broaddus, W. C.; Chen, Z. J.; Shu, C. Y.; Zhang, J. F.; Ge, J. C.; Dorn, H. C.; Corwin, F.; Hirsch, J. I.; Wilson, J.; Fatouros, P. P. Conjugation of functionalized gadolinium metallofullerenes with IL-13 peptides for targeting and imaging glial tumors. *Nanomedicine* **2011**, *6*, 449–458.

71 Shultz, M. D.; Wilson, J. D.; Fuller, C. E.; Zhang, J.; Dorn, H. C.; Fatouros, P. P. Metallofullerene-based nanoplatform for brain tumor brachytherapy and longitudinal imaging in a murine orthotopic xenograft model. *Radiology* **2011**, *261*, 136–143.

72 Shultz, M. D.; Duchamp, J. C.; Wilson, J. D.; Shu, C.-Y.; Ge, J.; Zhang, J.; Gibson, H. W.; Fillmore, H. L.; Hirsch, J. I.; Dorn, H. C.; Fatouros, P. P. Encapsulation of a radiolabeled cluster inside a fullerene cage, $^{177}Lu_xLu_{(3-x)}N@C_{80}$: An interleukin-13-conjugated radiolabeled metallofullerene platform. *J. Am. Chem. Soc.* **2010**, *132*, 4980–4981.

73 Ehrich, M.; Van Tassell, R.; Li, Y. B.; Zhou, Z. G.; Kepley, C. L. Fullerene antioxidants decrease organophosphate-induced acetylcholinesterase inhibition in vitro. *Toxicol. Vitro* **2011**, *25*, 301–307.

74 Liedtke, M.; Sperlich, A.; Kraus, H.; Baumann, A.; Deibel, C.; Wirix, M. J. M.; Loos, J.; Cardona, C. M.; Dyakonov, V. Triplet exciton generation in bulk-heterojunction solar cells based on endohedral fullerenes. *J. Am. Chem. Soc.* **2011**, *133*, 9088–9094.

75 Feng, L.; Rudolf, M.; Wolfrum, S.; Troeger, A.; Slanina, Z.; Akasaka, T.; Nagase, S.; Martin, N.; Ameri, T.; Brabec, C. J.; Guldi, D. M. A paradigmatic change: Linking fullerenes to electron acceptors. *J. Am. Chem. Soc.* **2012**, *134*, 12190–12197.

76 Bharadwaj, P.; Novotny, L. Plasmon-enhanced photoemission from a single $Y_3N@C_{80}$ fullerene. *J. Phys. Chem. C* **2010**, *114*, 7444–7447.

gadofullerene-based magnetic resonance imaging contrast agent with high ^{1}H relaxivity. *Bioconjugate Chem.* **2009**, *20*, 1186–1193.